Journal of Materials Science

Fabrication of high-performance wearable strain sensors by using CNTs coated electrospun polyurethane nanofibers

--Manuscript Draft--

Manuscript Number:	JMSC-D-20-03280R2
Full Title:	Fabrication of high-performance wearable strain sensors by using CNTs coated electrospun polyurethane nanofibers
Article Type:	Manuscript (Regular Article)
Keywords:	thermoplastic polyurethane; carbon nanotubes; electrospinning; Aligned; Strain sensor
Corresponding Author:	Liang Jiang Qingdao University Qingdao, -- Please Select -- CHINA
Corresponding Author Secondary Information:	
Corresponding Author's Institution:	Qingdao University
Corresponding Author's Secondary Institution:	
First Author:	Yuhao Wang
First Author Secondary Information:	
Order of Authors:	Yuhao Wang
	Wenyue Li
	Yanfen Zhou
	Liang Jiang
	Jianwei Ma
	Shaojuan Chen
	Stephen Jerrams
	Fenglei Zhou
Order of Authors Secondary Information:	
Abstract:	In this work, a new kind of composite nanofiber-based strain sensor with superior electromechanical properties was fabricated by using aligned thermal plastic polyurethane (TPU) nanofibers coated with multi-wall carbon nanotubes (CNTs). In order to improve the deposition efficiency and the fastness of CNTs coating on TPU nanofibers, bio-inspired dopamine (DA) was employed to modify the surface of the TPU nanofiber via a fast deposition method (the composite nanofibers obtained were denoted as DATPU). The electromechanical tests showed that DATPU/CNTs nanofiber membrane had a wide linear working range of 370% in the direction parallel to the nanofibers (P-DATPU/CNTs), a high gauge factor of 22.0 and a high linear coefficient of determination (r 2) of 0.997. P-DATPU/CNTs nanofibers also exhibited excellent durability during stretching-releasing test for 5000 cycles. The P-DATPU/CNTs composite nanofibers demonstrated high sensing performance in detecting human motions of finger and elbow bendings.
Funding Information:	National Natural Science Foundation of China (51703108) — Dr. Liang Jiang

Fabrication of high-performance wearable strain sensors by using CNTs coated electrospun polyurethane nanofibers

Yuhao Wang [a], Wenyue Li [a], Yanfen Zhou [a], Liang Jiang [a, *], Jianwei Ma [a], Shaojuan Chen [a], Stephen Jerrams [b], Fenglei Zhou [a, c]

[a] College of Textiles and Clothing, Qingdao University, Qingdao 266071, PR China

[b] Centre for Elastomer Research, Focas Research Institute, Dublin Institute of Technology, Dublin D08 NF82, Ireland

[c] Centre for Medical Image Computing, University College London, London, WC1V 6LJ, UK

Abstract: In this work, a new kind of composite nanofiber-based strain sensor with superior electromechanical properties was fabricated by using aligned thermal plastic polyurethane (TPU) nanofibers coated with multi-wall carbon nanotubes (CNTs). In order to improve the deposition efficiency and the fastness of CNTs coating on TPU nanofibers, bio-inspired dopamine (DA) was employed to modify the surface of the TPU nanofiber via a fast deposition method (the composite nanofibers obtained were denoted as DATPU). The electromechanical tests showed that DATPU/CNTs nanofiber membrane had a wide linear working range of 370% in the direction parallel to the nanofibers (P-DATPU/CNTs), a high gauge factor of 22.0 and a high linear coefficient of determination (r^2) of 0.997. P-DATPU/CNTs nanofibers also exhibited excellent durability during stretching-releasing test for 5000 cycles. The P-DATPU/CNTs composite nanofibers demonstrated high sensing performance in detecting human

* Corresponding author, E-mail: liang.jiang@qdu.edu.cn

motions of finger and elbow bendings.

Keywords: Thermoplastic polyurethane; Carbon nanotubes; Electrospinning; Aligned; Strain sensor

1 Introduction

In recent years, various wearable flexible electronic strain sensors, having the ability of monitoring the physiological state of the human body, such as limb movement, heartbeat and breathing, have attracted considerable interests [1-5]. Nanofiber-based flexible strain sensors have considered to be an excellent candidate to develop the next generation of wearable electronic products due to their advantages of large specific surface area, softness, lightness and ease of processing into complex structures. Generally, high-performance strain sensors should possess high sensitivity (suggested by gauge factor, GF), large working range and high stability [6-8]. Therefore, in order to obtain an excellent nanofiber-based strain sensor, ultra-high stretchable substrates with excellent electrically conductive media must be considered. To date, flexible polymers, such as thermoplastic polyurethane (TPU) [9,10], styrene butadiene styrene (SBS) [11,12] or polyvinylidene fluoride (PVDF) [13], etc., functionalized with conductive carbon materials, such as grapheme [14], carbon black [15] and carbon nanotubes (CNTs) [16,17], have been widely utilized in the preparation of nanofiber-based strain sensors.

Compared with traditional polymer film substrates, electrospun fibers have the advantages of large specific surface area, fine diameter and commendable mechanical flexibility, which could be used as ideal base materials for fabricating functional composites [18]. Especially, TPU could be easily electrospun into fibrous membrane, which displayed outstanding stretchability, flexibility and mechanical strength [19,20]. Lu et al. [21] prepared a sandwich-structure strain sensor by depositing silver nanowires

(AgNWs) on a TPU electrospun membrane and then spin-coated the composite with liquid polydimethylsiloxane (PDMS). This strain sensor exhibited a high sensitivity of gauge factor of 12.9 and an excellent reliability of 1600 cycles, while it had a low working range of 50% and low tensile strength of 2.8 MPa. Tong et al. [22] prepared a strain sensor by *in situ* polymerization of polyaniline (PANI) on an electrospun TPU nanofibrous membrane, which showed a high gauge factor of 6.7252 in a strain range from 0 to 120% and about 49.5060 among the strain ranging from 120 to 150% with a low working range of 160% and low tensile strength of 1.93 MPa. Yang et al. [23] fabricated a flexible strain sensor by coating an electrospun TPU mat with 2D transition metal carbides and nitrides (MXene) sheets, the strain sensor possessed the excellent properties of high gauge factor of 228, low detection limits of 0.1%, but the working range was only 150%. Therefore, the strain sensors based on conventional random electrospun nanofibers have relatively narrow working range and/or a low mechanical strength, which have limited the practical application of strain sensors. In order to improve the mechanical strength of electrospun nanofibers, novel electrospinning technologies have been explored to obtain aligned nanofibers by employing a high speed rotating collector [24], applying two pairs of copper (Cu) electrodes as the collector [25], using magnetic-field-assisted electrospinning [26] or using near-field electrospinning [27]. Owing to the highly aligned structure, the membranes prepared exhibited superior mechanical properties [28-30]. In addition, it has been reported that one-dimensional structured multi-wall CNTs possessing high electrical conductivity and superior mechanical [16,31] composited with SBS fibers has been used for fabricating strain sensors with improved working range and durability [32].

This study aims to fabricate a kind of flexible strain sensors with large working range, excellent sensitivity and high mechanical strength by using highly aligned

electrospinning TPU nanofibers coated with CNTs. In order to improve the deposition efficiency and fastness of CNTs coating, dopamine, which has been used widely for the surface modification of various organic/inorganic materials with improved interfacial strength [33-35], was used to modify electrospun TPU nanofibers. The dopamine depositing rate on TPU nanofibers was drastically accelerated by using $NaIO_4$. The sensing behavior of composite nanofiber membranes stretching on the direction parallel to the nanofiber and vertical to the nanofiber was investigated in this study, respectively. The sensing stability, durability and washing fastness of the composite nanofibers were also studied. Finally, a prototype of strain sensor was constructed from DATPU/CNTs composite nanofibers and used to detect finger and elbow bendings.

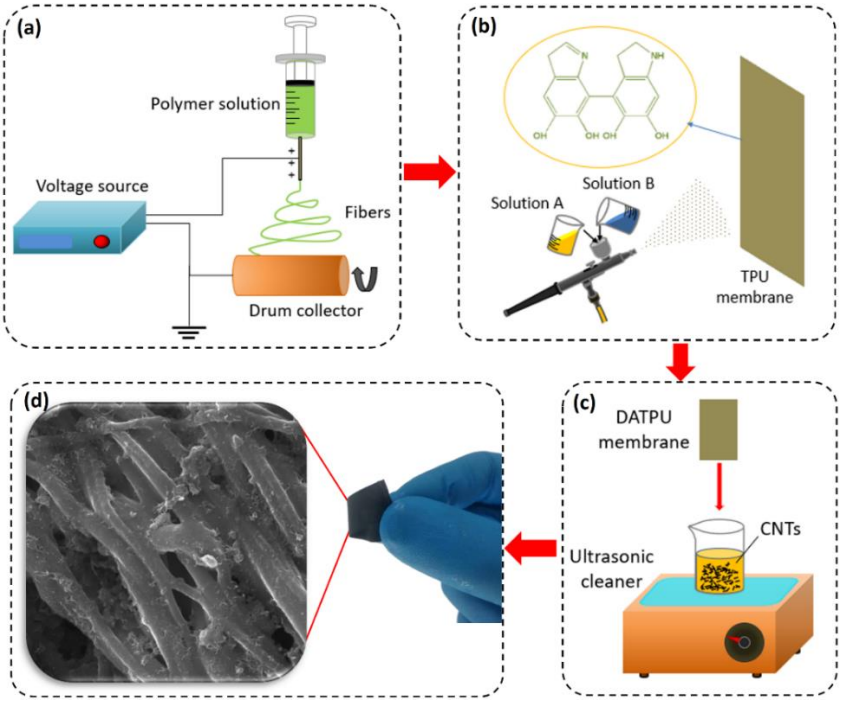

Figure 1. Illustration of the procedure for preparing composite nanofibers: (a) The schematic of fabricating aligned TPU nanofibers; (b) The schematic of DA modifying aligned TPU nanofibers; (c) The schematic of CNTs coating DA modified aligned TPU nanofibers; (d) The morphology of a DATPU/CNTs nanofibers.

2 Experimentation

2.1 Materials

Polyester-based polyurethane (TPU) was purchased from Shandong INOV New Materials Co., Ltd. (Zibo, Shandong, China). Tetrahydrofuran (THF), N, N-dimethylformamide (DMF) and sodium hydroxide (NaOH) were purchased from Sinopharm Chemical Reagent Co., Ltd. (Shanghai, China). Dopamine hydrochloride (DA·HCl) and Sodium periodate ($NaIO_4$) were produced from Shanghai Macklin Biochemical Co., Ltd. (Shanghai, China). Tris (hydroxymethyl) aminomethane (Tris) was purchased from Beijing Solarbio Science & Technology Co., Ltd. (Beijing, China) and multi-wall carbon nanotubes (CNTs) were acquired from Cnano Technology (Beijing China).

2.2 Preparation of aligned electrospun TPU nanofibers

The procedure for preparing aligned electrospun TPU nanofibers is depicted in Figure 1(a). TPU pellets were dried in a vacuum oven at 80 °C for 24 h to remove the absorbed moisture before use. Firstly, the pellets with a weight concentration of 18% were dissolved in a mixed solvent of DMF and THF having the volume ratio of 1:3. The mixture was magnetically stirred at 60 °C for 1 h to accelerate the dissolving and then stirred for another 6 h at room temperature to ensure complete dissolving. In order to fabricate the electrospun TPU nanofibers, the TPU solution was loaded in a plastic syringe (10 mL) connected to a 22 gauge blunt end needle and the syringe was mounted on a digital syringe pump (Longer Precision Pump Co., Ltd., Baoding, Hebei, China). The electrospinning procedure was carried out under the temperature of 20 °C and the humidity of 25% using the following process parameters: applied voltage of 20 kV, working distance of 20 cm between the capillary tip and the collector and solution flow rate of 4 mL h^{-1}. The TPU nanofibers with different degree of alignment were obtained by changing the rotating drum collector speed. Finally, the resultant TPU nanofiber membranes were left in a fume hood overnight at room temperature to remove the

remaining solvent. TPU nanofibers, parallel and vertical to the nanofiber direction, are defined as P-TPU and V-TPU respectively.

2.3 Dopamine modification of electrospun TPU nanofibers

For surface modification of electrospun TPU nanofibers, a 2.0 g L^{-1} aqueous solution of dopamine (DA) was initially prepared by dissolving DA·HCl powder in distilled water and the pH of the solution was buffered to 8.5 by adding Tris and NaOH; $NaIO_4$ solution with a concentration of 30 mM was added to the above dopamine solution to form a mixed solution of DA/$NaIO_4$. The mixture was immediately sprayed onto the TPU nanofibers, and then the color of the solution quickly changed from light pink to dark brown with the spontaneous deposition of an adherent polydopamine (PDA) layer (Figure 1(b)). After 2 h, the TPU nanofibers were washed with deionized water and dried at 60 °C in a vacuum. The resultant TPU nanofibers were denoted as DATPU.

2.4 Preparation of CNTs coated TPU nanofibers

Firstly, CNTs suspension was prepared by adding 40 mg CNTs in 40 mL deionized water. Both pristine TPU and DATPU nanofiber membranes with size of 40 mm × 10 mm were immersed into the above CNTs suspension. After treatment under ultrasonication for 60 min, the CNTs coated pristine TPU and DATPU nanofiber membranes were taken out from the beaker, washed with deionized water three times and dried in a vacuum oven at 60 °C for 24 h. The CNTs coated pristine TPU and DATPU nanofibers were termed as TPU/CNTs and DATPU/CNTs, respectively.

2.5 Characterization

The morphology of aligned TPU nanofibers and composite nanofibers were observed using a Scanning Electron Microscope (SEM) (Tescan Vega3, Brno, Czech Republic). The samples were coated with a thin layer of gold prior to the observation and SEM images with different magnifications were taken at an accelerated voltage of 10 kV. The

angle distribution (relative to longitudinal axis) was determined and the average nanofiber diameter was measured with ImageJ software from 100 random nanofibers in the SEM images.

Tensile tests were carried out on a tensile testing machine (Instron-3300 Tensile Machine, Glenview, US) under standard conditions (25 °C/65% RH) with an uniaxial tensile force applied at a speed of 100 mm min^{-1}. The size of each specimen was 10 mm in width and 20 mm in length. The elastic modulus (*Y*) was calculated from the slope of the stress-strain curve in the strain range of 0-10%. Each sample was tested three times under the same conditions, and the average value from the three tests was used.

The water contact angle (WCA) of electrospun TPU and DATPU nanofiber membranes was measured by employing a water contact angle meter from Krüss DSA100 (Germany) with a drop volume of 2 μL. Each sample was tested at least three times in different positions and the average WCA was used.

The surface chemical structure of aligned TPU and DATPU nanofibers was determined using Fourier transform infrared spectroscopy (FTIR) (Nicolet 5700, Massachusetts, US). The spectrum was collected in the wave number range from 4000 cm^{-1} to 400 cm^{-1} at scanning times of 32 and resolution of 4 cm^{-1}.

Thermogravimetric analysis was carried out using a DSC/TG synchronous thermal analyzer (STA449 F3 Jupiter, Bavaria, Germany). The measurements were conducted under a nitrogen atmosphere. The sample, with a weight of about 5 mg, was heated from ambient temperature to 800 °C with a heating rate of 20 °C min^{-1}.

The resistance of TPU/CNTs and DATPU/CNTs composite nanofibers was investigated by using a digital multimeter (KEYSIGHT B2901A, US) which was equipped with a stepper motor to induce various deformations in the tested samples. The nanofiber membrane with a size of 20 mm × 10 mm was connected with the copper tapes, which

served as electrodes during the testing. To ensure good contact between the copper tape and the sample under test, both ends of the TPU/CNTs and DATPU/CNTs strips were coated with silver paste.

Sheet resistance of TPU/CNTs and DATPU/CNTs composite nanofibers was measured by employing a multifunction digital four-probe tester (ST-2258C, Jiangsu, China) with the current of 1 mA. The experimental data point of sheet resistance was the average of the results obtained from at least five samples tested under the same condition.

3 Results and Discussion

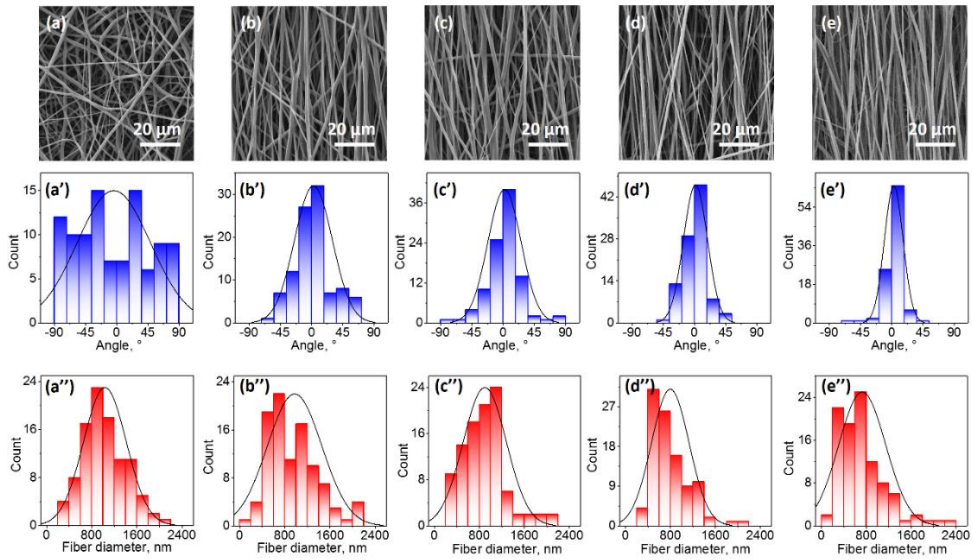

Figure 2. SEM photographs of electrospun TPU nanofibers collected with different collector rotation speeds: (a) 250 rev min^{-1}; (b) 1500 rev min^{-1}; (c) 2500 rev min^{-1}; (d) 3500 rev min^{-1}; (e) 4500 rev min^{-1}; Angular distribution of electrospun TPU nanofibers and fit by a Gaussian curve: (a') 250 rev min^{-1}; (b') 1500 rev min^{-1}; (c') 2500 rev min^{-1}; (d') 3500 rev min^{-1}; (e') 4500 rev min^{-1}; Nanofiber diameter distribution and fit by a Gaussian curve: (a") 250 rev min^{-1}; (b") 1500 rev min^{-1}; (c") 2500 rev min^{-1}; (d") 3500 rev min^{-1}; (e") 4500 rev min^{-1}.

The surface morphology of electrospun TPU nanofibers collected with different rotation speeds is shown in Figure 2. It can be seen from Figure 2(a) and (a') that when

the rotating speed of the drum collector was 250 rev min^{-1}, the nanofibers distributed in a random manner in the membrane. As shown in Figure 2(b), (b'), (c), (c'), (d), (d'), (e), and (e'), the angles of the nanofibers relative to longitudinal axis for all obtained electrospun TPU nanofibers were almost formed within an angle range from -18 ° to 18 ° with increasing drum speed from 1500 rev min^{-1} to 4500 rev min^{-1}, indicating a highly aligned distribution. Additionally, it was found that the average nanofiber diameter was decreased with increasing in rotating speed of the collector as shown in Figures 2(a''), (b''), (c''), (d'') and (e''). For example, the nanofibers obtained at a collector speed of 250 rev min^{-1} had an average diameter of 1033 ± 380 nm, while nanofiber diameter reduced from 972 ± 480 nm to 726 ± 416 nm when the collector speed was increased from 1500 rev min^{-1} to 4500 rev min^{-1}. This is primarily because when the nanofibers reached the high-speed rotating collector, they attached to the collector by an electrostatic force and were further stretched, finally resulting in a reduction in diameter and the formation of aligned nanofibers from the induced spiraling path [36-38]. The higher the collector speed, the greater the stretching force received by the nanofibers and the higher the degree of alignment [39].

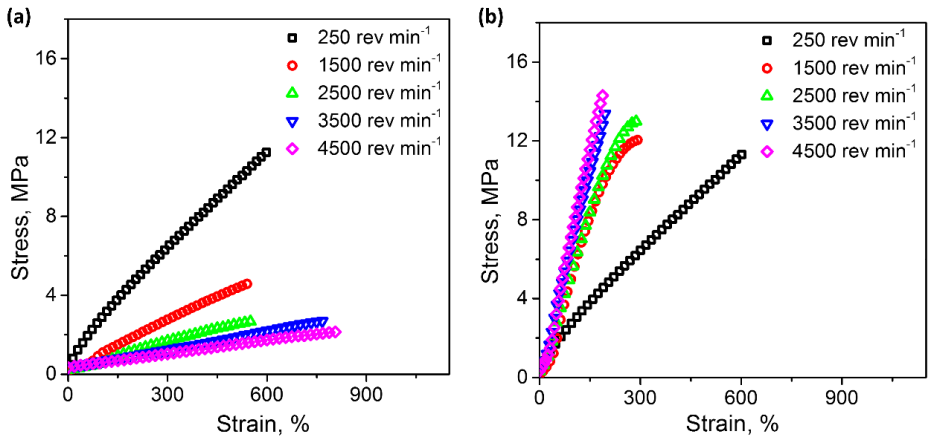

Figure 3. Stress-strain curves of: (a) TPU nanofiber membranes subjected to tensile tests in a direction vertical to the nanofibers and (b) TPU nanofiber membranes subjected to tensile tests in a direction parallel to the nanofibers at different collector rotating speeds.

Table 1 Mechanical properties of P-TPU nanofibers and V-TPU nanofibers: elastic modulus (E), tensile strength (σ) and elongation at break ($\varepsilon_{at\ break}$)

	P-TPU nanofibers			V-TPU nanofibers		
	E (MPa)	σ (MPa)	$\varepsilon_{at\ break}$ (%)	E (MPa)	σ (MPa)	$\varepsilon_{at\ break}$ (%)
250 rev min^{-1}	3.70 ± 0.22	11.21 ± 0.10	592 ± 26	3.67 ± 0.25	11.07 ± 0.16	612 ± 22
1500 rev min^{-1}	4.31 ± 0.13	12.09 ± 0.35	293 ± 13	0.57 ± 0.04	3.65 ± 0.22	671 ± 78
2500 rev min^{-1}	8.58 ± 0.73	12.18 ± 1.22	247 ± 83	0.57 ± 0.02	3.45 ± 0.25	611 ± 6
3500 rev min^{-1}	10.08 ± 0.09	13.32 ± 1.07	194 ± 11	0.56 ± 0.06	2.42 ± 0.47	941 ± 67
4500 rev min^{-1}	10.29 ± 0.16	14.60 ± 0.51	192 ± 15	0.50 ± 0.10	1.80 ± 0.26	940 ± 85

As is well known, the mechanical performance is of vital importance for engineering materials to realize various applications. Figure 3 shows the typical stress-strain curves of electrospun TPU nanofiber membranes obtained at various collector rotating speeds. The corresponding tensile strength, elongation at break and elastic modulus for each material were summarized in Table 1. As can be seen from Figure 3 and Table 1, for random TPU nanofiber membranes, which were collected at 250 rev min^{-1}, the tensile strength and elongation at break showed slight difference when stretched in vertical and parallel directions. For aligned TPU nanofiber membranes with the drum rotating speed of 1500 rev min^{-1} and above 1500 rev min^{-1}, the tensile strength of P-TPU was higher while the elongation at break of V-TPU was higher. Furthermore, mechanical properties changed regularly with the collected speed increasing, for example, when the collector

speed increased from 1500 rev min^{-1} to 4500 rev min^{-1}, the tensile strength of V-TPU decreased from 3.65 ± 0.22 MPa to 1.80 ± 0.26 MPa, the elastic modulus decreased from 0.57 ± 0.04 MPa to 0.50 ± 0.10 MPa and the elongation at break increased from 611 ± 6% to 941 ± 67%. However, for P-TPU, when the collector speed increased from 1500 rev min^{-1} to 4500 rev min^{-1}, there was a pronounced increase in tensile strength from 12.09 ± 0.35 MPa to 14.60 ± 0.51 MPa, the elastic modulus from 4.31 ± 0.13 MPa to 10.29 ± 0.16 MPa, and the elongation at break from 192 ± 15% to 293 ± 13%. It is attributed that the high-speed rotating drum collector imparted a large stretching force to the nanofibers, which increased the degree of molecular chain alignment in the nanofibers and consequently enhanced their tensile strength [40,41]. Moreover, TPU nanofibers collected at low rotating speeds were expected to exhibit irregularly distributed hard segments, whereas hard segments of stretched nanofibers collected at high collector speeds exhibited periodic changes in structure along the stretching direction [42], leading to an increase in elastic modulus.

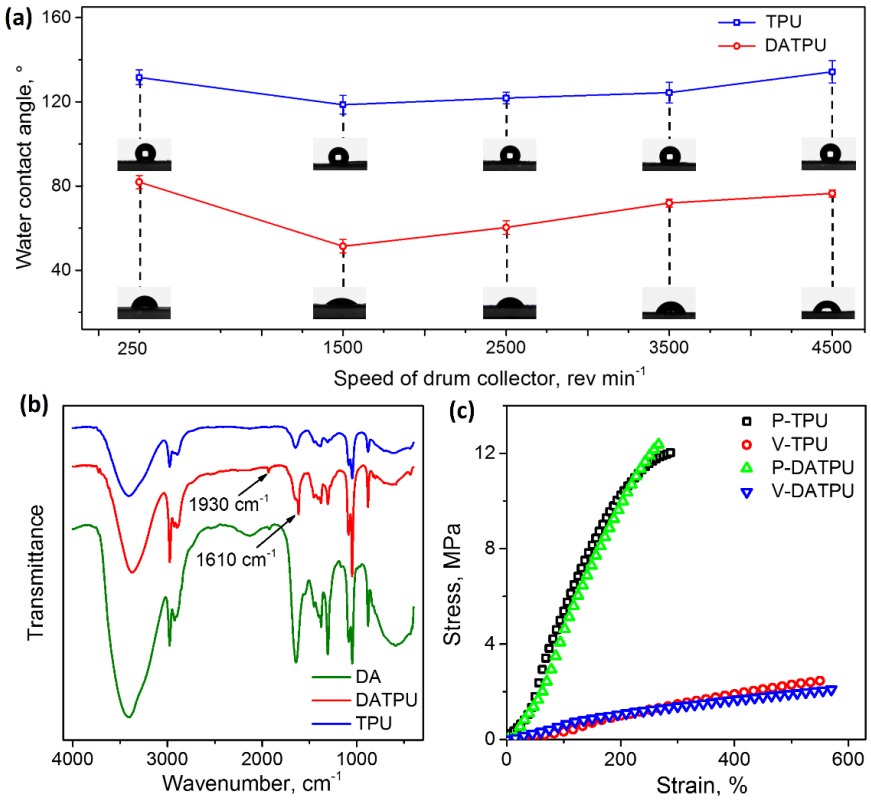

Figure 4. (a) The curves of water contact angle (WCA) versus rotating speed for TPU and DATPU nanofiber membranes; (b) FTIR spectra of reagent sample of DA, TPU and DATPU nanofiber membranes; (c) Stress-strain curves of TPU and DATPU nanofiber membranes prepared at a speed of 1500 rev min^{-1}.

Since the decoration of TPU nanofiber membranes with CNTs was performed in an aqueous solution, the hydrophilic properties of the nanofiber membranes would have a non-negligible effect on the deposition of CNTs. More CNTs in the suspension could infiltrate into the aperture in the electrospun membranes with good hydrophilicity, ensuring a high deposition efficiency. Taking this into consideration, the hydrophilic property of TPU and DATPU nanofiber membranes obtained at different drum collector speed was investigated in Figure 4(a). It can be seen from Figure 4(a) that the WCA of all TPU nanofiber membranes exceeded 117 °, indicating the hydrophobic behavior for these materials. Specifically, TPU nanofiber membranes obtained at a collector rotating speed of 1500 rev min^{-1} had the lowest WCA of 117 ± 4 ° while the membrane obtained at a collector rotating speed of 4500 rev min^{-1} showed the highest WCA of 136 ± 5 °. Generally, for thinner nanofibers, the wicking effect, acting to absorb or draw off liquid by capillary action, could become significant, which contributed to the decrease of WCA [43]. However, with a decrease in the nanofiber diameter, the specific surface area became larger, leading an increase WCA of nanofiber membrane [44]. Therefore, when the nanofibers were collected at a rotating speed below 1500 rev min^{-1}, the wicking effect dominated, resulting in relatively higher hydrophobicity. When the nanofibers were collected at rotating speeds above 1500 rev min^{-1}, the effect of specific surface area dominated and hydrophilicity gradually decreased as increasing collector rotating speeds.

In order to improve the hydrophilicity of electrospun TPU nanofiber membranes, rapid polydopamine deposition with the assistance of oxidant $NaIO_4$ was employed to modify

the surface of the TPU nanofiber membranes. The WCA of all TPU nanofiber membranes obtained at different collector speeds remarkably decreased after polydopamine modification shown in Figure 4(a). This is because the hydroxyl and amino groups in the PDA molecule improved the hydrophilicity of the TPU nanofiber membranes. Particularly, the WCA of the TPU nanofiber membranes obtained at a collector rotating speed of 1500 rev min^{-1} decreased from 117 ± 4 ° to 51 ± 3 ° after polydopamine modification. This was expected to greatly benefit for the efficient deposition of CNTs on TPU nanofiber membranes.

Due to the fact that both TPU and dopamine contain amide group, it is unlikely to determine the source of this group by using FTIR analysis. Thus, TPU and DATPU nanofibers were firstly washed with sodium hydroxide ethanol solution to get reagent samples, respectively. Then, the FTIR analysis for the reagent samples was carried out to confirm whether dopamine successfully modified the TPU nanofibers. As shown in the FTIR spectrum of the reagent samples in Figure 4(b), a new peak at 1610 cm^{-1} represented the C=C stretching vibration of the aromatic ring and the bending vibration of N–H, indicating that the surface of DATPU nanofibers was introduced a hydrophilic group of –NH [45]. In addition, compared with the washing solution of TPU nanofibers, a new peak at 1930 cm^{-1}, which was ascribed to the C=C stretching vibration of benzene derivative, emerged in the FTIR spectrum of reagent sample of both DATPU and DA. The above results confirmed the successful deposition of PDA on the TPU nanofibers. As shown in Figure 4(c), the tensile strength and elongation at break of TPU nanofiber membranes scarcely changed after dopamine modification.

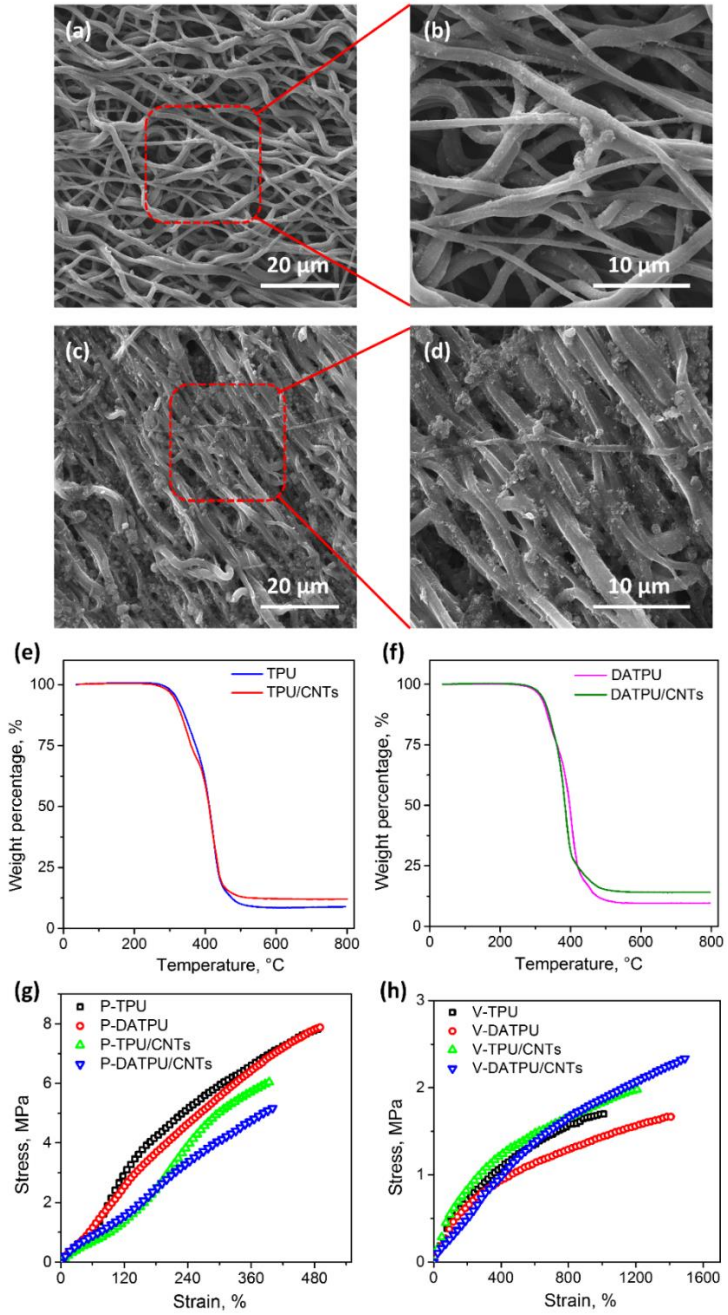

Figure 5. **(a-b) Surface morphology of TPU/CNTs; (c-d) Surface morphology of DATPU/CNTs; (e) TGA curves of TPU and TPU/CNTs; (f) TGA curves of DATPU and DATPU/CNTs; (g) Stress-strain curves of P-TPU, P-DATPU, P-TPU/CNTs and P-DATPU/CNTs nanofiber membranes at a stretch rate of 10 mm min^{-1}; (h) Stress-strain curves of V-TPU, V-DATPU, V-TPU/CNTs and V-DATPU/CNTs nanofiber membranes at a stretch rate of 10 mm min^{-1}.**

Because the electrospun TPU membrane prepared at 1500 rev min^{-1} had highly aligned structure, reliable tensile strength in both directions and good hydrophilicity after

dopamine modification, it was selected to be used as the substrate for constructing CNTs coated conductive nanofiber membranes. Figure 5(a-d) shows the surface morphology of TPU/CNTs and DATPU/CNTs respectively. It can be seen that for both TPU/CNTs and DATPU/CNTs composites, CNTs were successfully deposited on the surface of the nanofibers. This is because CNTs were rapidly pushed towards to the surface of outer nanofibers and through the pores to the surface of inner nanofibers with high energy during ultrasonication and subsequently interfacial collision occurred. As a result, the nanofibers might become softened or even partially melt leading to CNTs tightly anchored onto the nanofibers surface [46]. Besides, because of the stretching force induced by high rotating collector, nanofibers exhibited straighten stage during the electrospinning procedure, after releasing from the collector, the nanofibers became curved.

TGA was employed to analyze the amount of CNTs coated on both the pristine TPU nanofibers and the DATPU nanofibers. As seen from Figure 5(e) and (f), when the temperature reached 800 °C, the weight loss of the pristine TPU nanofibers was 91.1%, while the TPU/CNTs was 88.0%; the weight loss rate of DATPU nanofibers was 90.4% and after coated with CNTs, the weight loss rate of DATPU/CNTs was 86.0%. Thus, the content of CNTs on the pristine TPU nanofibers and DATPU nanofibers was 3.1% and 4.4%, respectively, revealing the effect of polydopamine modification.

The mechanical properties of TPU, DATPU, TPU/CNT and DATPU/CNT were investigated. It can be seen in Figure 5(g) that after CNTs coated on the substrate, both the tensile strength and the elongation at break in the nanofiber direction were reduced. The tensile strength and elongation at break of P-TPU were 7.76 ± 0.21 MPa and 478 ± 30% respectively, while those of P-TPU/CNTs were 6.04 ± 0.13 MPa and 394 ± 7% respectively. After polydopamine modification, the tensile strength and elongation at

break of P-DATPU were 7.84 ± 0.17 MPa and 484 ± 25% respectively, while those of P-DATPU/CNTs were 5.23 ± 0.26 MPa and 406 ± 19% respectively. The reason why after coated with CNTs, the tensile strength of P-TPU/CNTs and P-DATPU/CNTs decreased is probably that the ultrasonic power damaged the nanofibers [47]. However, the elongation at break and tensile strength in the vertical nanofiber direction were mostly improved compared with those in the nanofiber direction. As is illustrated in Figure 5(h), the elongation at break and tensile strength of V-TPU were 992 ± 28% and 1.70 ± 0.07 MPa respectively, while those of V-DATPU were 1399 ± 38% and 1.67 ± 0.12 MPa. With the deposition of CNTs, the elongation at break and tensile strength of V-TPU/CNTs were 1206 ± 26% and 1.98 ± 0.14 MPa, while those of V-DATPU/CNTs were 1491 ± 34% and 2.34 ± 0.10 MPa. The probable reason behind the improvement in mechanical properties is that well coated CNTs had a strong interaction with nanofibers, bridging the neighboring nanofibers [48].

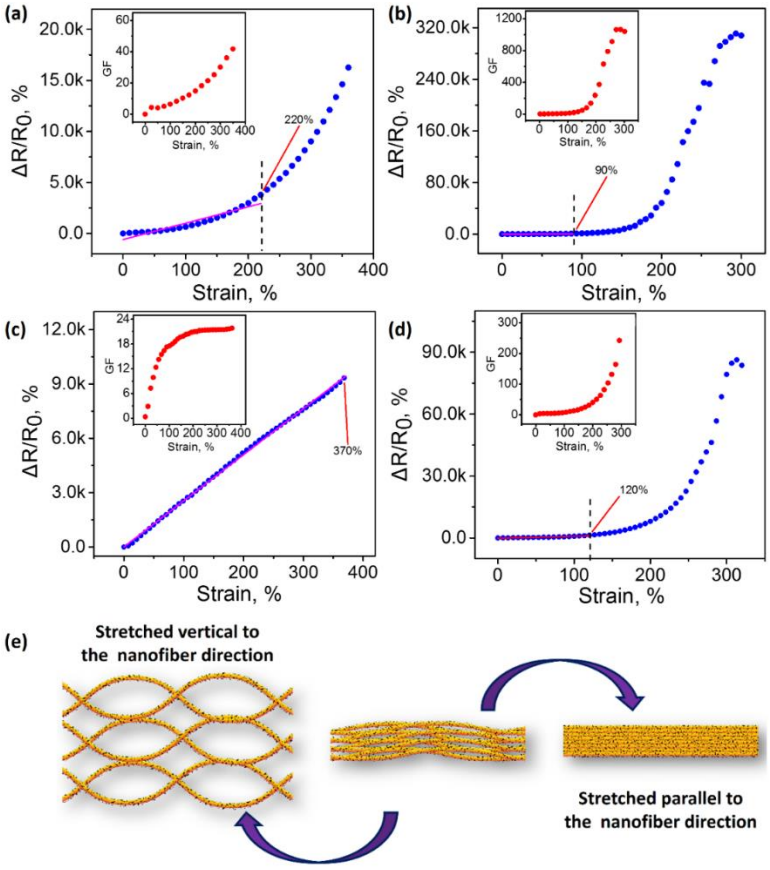

Figure 6. The relative resistance ($\triangle R/R_0$) and gauge factor (GF) versus applied strain of composite nanofibers during ultimate tensile tests at a 10 mm min^{-1} stretch rate: (a) P-TPU/CNTs; (b) V-TPU/CNTs; (c) P-DATPU/CNTs; (d) V-DATPU/CNTs. Insets show the gauge factor; (e) Schematic of the structure change of the composite nanofibers stretched vertical to the nanofiber direction and parallel to the nanofiber direction.

In order to determine the sensing behavior of the conductive composite nanofibers, electromechanical experiments were carried out at a stretch rate of 10 mm min^{-1}. Generally, the relative resistance ($\triangle R/R_0$, $\triangle R = R-R_0$, where R_0 is the initial resistance and R represents the real-time resistance) and gauge factor (GF = $(\triangle R/R_0)/\varepsilon$, where ε is the strain in the samples) were used for evaluating the electromechanical properties of conductive composite nanofibers. The high linearity is also significant because it simplifies the calibration processes and enhances the accuracy of measurements [8]. In this study, the coefficient of determination (r^2) was used to characterize the linearity of strain sensors and the maximum working range of the strain sensor was determined as the strain at which the resistance reached the limit to be measured by the digital multimeter [11]. It is well known that when the value of r^2 is larger than 0.9, the data has an excellent correlation with the linear model [49]. It can be seen from Figure 6(a) that the maximum working range of P-TPU/CNTs was 365%, with a GF of 47.1. In addition, P-TPU/CNTs had good linearity in the strain range from 0% to 220%. As demonstrated in Figure 6(b) that the maximum working range (295%) of V-TPU/CNTs was much narrower compared to that of P-TPU/CNTs, while the GF (1053.7) was larger than that of P-TPU/CNTs. A linear working range with $r^2 > 0.9$ for V-TPU/CNTs was observed in the strain range from 0% to 90%. The sensing behavior of P-DATPU/CNTs is shown in Figure 6(c). The maximum working range of P-DATPU/CNTs was 370% with excellent linearity ($r^2 = 0.997$) and a GF of 22.0. As shown in Figure 6(d), the maximum working range of V-DATPU/CNTs was in a strain range of 0% to 305% with

a linearity working range of 0% to 120%, and GF was 276.5. By analyzing the above results, it can be concluded that conductive composite nanofibers stretched in the direction vertical to nanofiber alignment had higher sensitivity, while stretched in a parallel direction had wider and more stable linear working range. The explanation for the phenomenon might be that as the substrates deformed in different forms, the conductive network of CNTs also presented different types of changes. As schematically shown in Figure 6(e), during the stretching process in the direction vertical to the nanofiber, wider "gaps" appeared and led to an increase in the distance between CNTs adsorbed on the surface of nanofibers, consequently resulting in a decrease in conductivity [14]. Owing to the large changes in resistance caused by small strain in the vertical direction, high GF was produced. Conversely, when the membrane was stretched along the nanofiber direction, the nanofibers were straightened and became compact, forming stable and excellent conductive paths which would induce smaller change in electrical resistance and as a consequence, a lower sensitivity was obtained. Based on the evaluation above, conductive composite nanofibers applied in the parallel direction were more reliable in keeping with the work requirements of strain sensors.

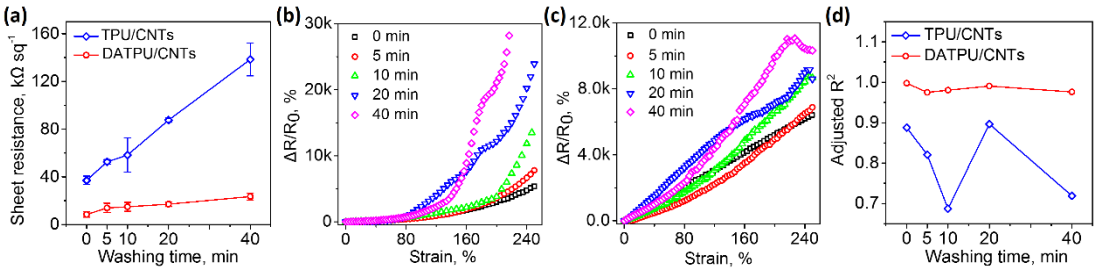

Figure 7. (a) Curves of sheet resistance with washing time of TPU/CNTs and DATPU/CNTs; Sensing behavior of composite nanofibers for 250% strain after washing for different periods of time: (b) TPU/CNTs; (c) DATPU/CNTs; (d) Curves of linearity with washing time of TPU/CNTs and DATPU/CNTs.

In order to investigate the washing fastness of P-TPU/CNTs and P-DATPU/CNTs

nanofibers, they were washed in a high-power ultrasonic cleaner filled with water for different time periods of 5 min, 10 min, 20 min and 40 min. The corresponding strain sensing behavior after washing is shown in Figure 7. As the washing time increased from 5 min to 40 min, the sheet resistance of P-TPU/CNTs exhibited a remarkable increase from 37.1 ± 3.4 kΩ sq^{-1} to 138.5 ± 13.8 kΩ sq^{-1} (Figure 7(a)) and r^2 showed an extremely unstable trend (Figure 7(b) and 7(d)). In the case of P-DATPU/CNTs, after being washed for 40 min, sheet resistance increased from 8.44 ± 2.2 kΩ sq^{-1} to 23.5 ± 2.8 kΩ sq^{-1} with the r^2 always changed in the range of 0.975-0.997, exhibiting a relatively stable trend (Figure 7(a), 7(c) and 7(d)). It can be concluded that the dopamine modification can greatly improve the washing fastness of conductive composite nanofibers.

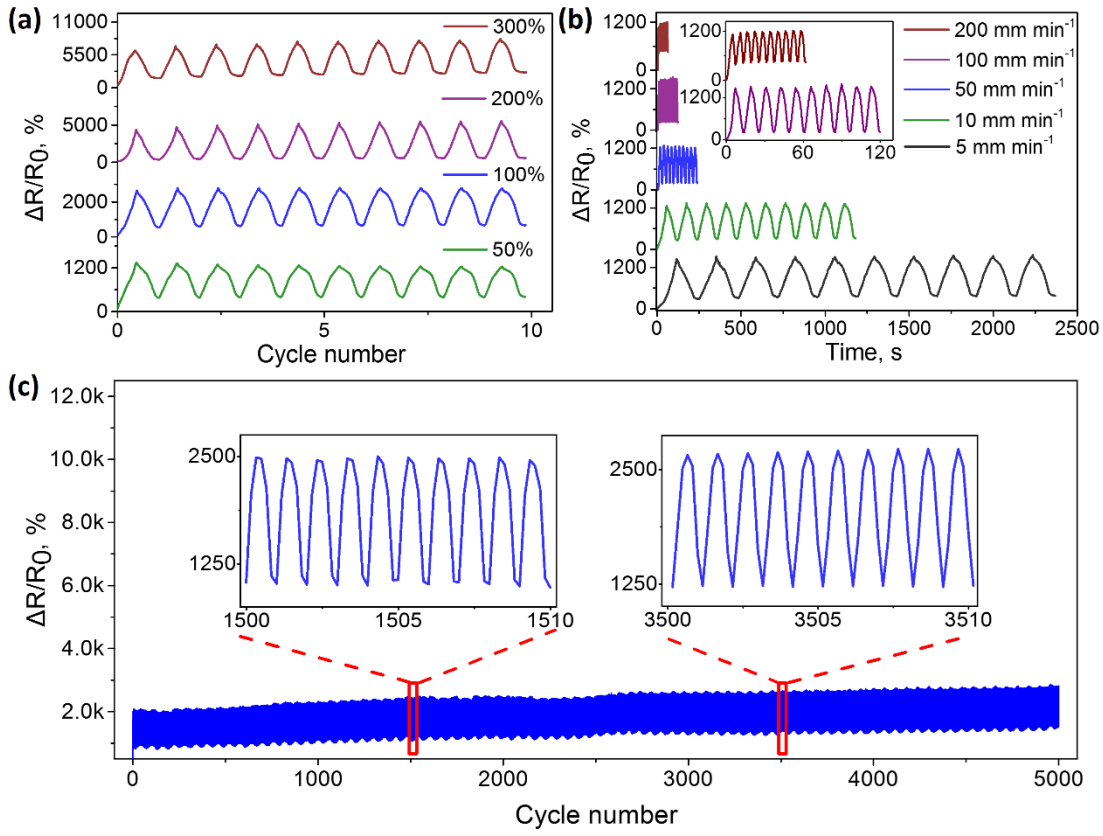

Figure 8. (a) Curves of relative resistance related to 10 stretching/releasing tests applied over different strain ranges: 0%-50%, 0%-100%, 0%-200%, and 0%-300% with a constant stretch rate of 10 mm min^{-1}; (b) Curves of relative resistance under 50% strain at the stretch rate of 5

mm min^{-1}, 10 mm min^{-1}, 50 mm min^{-1}, 100 mm min^{-1}, 200 mm min^{-1} for 10 cycles of stretching/releasing test; (c) Performance of a P-DATPU/CNTs during 5000 stretching-releasing tests over a strain range of 0% to 100%, indicating durability, insets are the sensing behavior in the ranges 1500-1510 and 3500-3510 cycles.

The working stability of P-DATPU/CNTs at different levels of strain and stretch rate were also studied. As shown in Figure 8(a), P-DATPU/CNTs exhibited excellent reproducibility and stability in different strain levels, indicating excellent adaptability in practical applications. Figure 8(b) shows the sensing behavior of P-DATPU/CNTs under 50% strain at different stretching/releasing rates of 5 mm min^{-1}, 10 mm min^{-1}, 50 mm min^{-1}, 100 mm min^{-1}, and 200 mm min^{-1} for 10 stretching-releasing test cycles. It can be seen that the P-DATPU/CNTs exhibited similar relative resistance changes under different stretch rates, confirming their ability to detect different external stimuli. The long-term sensing behavior of P-DATPU/CNTs is shown in Figure 8(c). Under a strain of 100% and a stretch rate of 10 mm min^{-1} for 5000 cycles, P-DATPU/CNTs still exhibited good stability during the stretching-releasing tests. For example, the relative resistance of P-DATPU/CNTs in 1500-1510 cycles was about 2500%, while that in 3500-3510 cycles was about 2650%, indicating excellent durability of CNT conductive network.

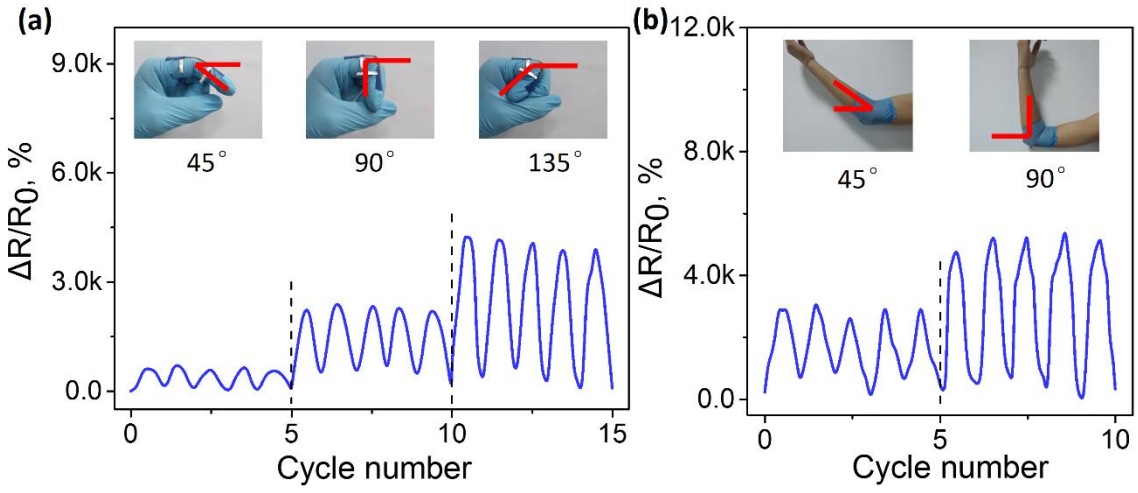

Figure 9. Relative resistance of P-DATPU/CNTs resulting from human motion: (a) Finger

bending for 5 cycles at different angles of 45 °, 90 °, 135 °; (b) Elbow bending for 5 cycles at different angles of 45 °, 90 °.

With the outstanding stretchability, sensitivity and reliability, P-DATPU/CNTs conductive composite nanofibers prepared in this work were used for the human motions detecting of the finger and elbow bendings. In this section, the participants were informed what they were asked to do in this experiment, then read and signed a consent form. As expected, the bendings of the finger and elbow were accurately detected by the P-DATPU/CNTs. It can be clearly seen from Figure 9 that as the bending degree of the finger increased from 0 ° to 45 °, 0 ° to 90 ° and 0 ° to 135 °, the relative resistance changed accordingly with the value of 632% , 2513% and 4135%, respectively. Similarly, with elbow bendings at two different angles of 45 ° and 90 °, the signals of relative resistance obtained were about 2822% and 5254%, corresponding to the detection angles.

4 Conclusions

In this paper, aligned electrospun TPU nanofibers based stain sensors were prepared by integrating with CNTs. The deposition amount of CNTs and the binding between CNTs and the TPU nanofibers were improved by employing a rapid dopamine modification method assisted with $NaIO_4$. The CNTs coated TPU nanofiber membrane with dopamine modification (DATPU/CNTs) had a 370% linear working range with r^2 of 0.997 together with excellent working stability in the direction parallel to the nanofibers. Additionally, it maintained good electrical properties even after 40 min ultrasonic washing and presented excellent durability with 5000 cycles of stretching-releasing test for sensing behavior. Both human finger and elbow bendings were accurately monitored by P-DATPU/CNTs based strain sensors. The developed P-DATPU/CNTs composite nanofibers have clearly demonstrated the great potential to be used for developing wearable strain sensors.

Acknowledgements

The authors gratefully acknowledge the National Natural Science Foundation of China (Grant no. 51703108), the National Key Research and Development Program of China (Grant no. 2017YFB0309805-2), the Shandong Provincial Natural Science Foundation, China (Grant no. ZR2017BEM042, ZR2018JL021), the Shandong Provincial Key Research and Development Program, China (Grant no. 2018GGX108003), Youth Innovation Science and Technology Plan of Shandong Province (Grant no. 2020KJA013) and Shandong "Taishan Youth Scholar Program" for financial support.

References

1. Li Y, Samad YA, Taha T, Cai G, Fu S, Liao K (2016) Highly Flexible Strain Sensor from Tissue Paper for Wearable Electronics. ACS Sustainable Chemistry & Engineering 4 (8):4288-4295

2. Gang G, Wei H, Shao J, Dong X (2018) Recent progress of flexible and wearable strain sensors for human-motion monitoring. Journal of Semiconductors 39 (1):011012

3. Liao X, Liao Q, Yan X, Liang Q, Si H, Li M, Wu H, Cao S, Zhang Y (2015) Flexible and Highly Sensitive Strain Sensors Fabricated by Pencil Drawn for Wearable Monitor. Advanced Functional Materials 25 (16):2395-2401

4. Li Y, Huang P, Zhu W, Fu S, Hu N, Liao K (2017) Flexible wire-shaped strain sensor from cotton thread for human health and motion detection. Scientific Reports 7 (1):45013

5. Li W, Zhou Y, Wang Y, Li Y, Jiang L, Ma J, Chen S (2020) Highly Stretchable and Sensitive SBS/Graphene Composite Fiber for Strain Sensors. Macromolecular

Materials and Engineering 305 (3):1900736

6. Song Z, Li W, Bao Y, Han F, Gao L, Xu J, Ma Y, Han D, Niu L (2018) Breathable and Skin-Mountable Strain Sensor with Tunable Stretchability, Sensitivity, and Linearity via Surface Strain Delocalization for Versatile Skin Activities' Recognition. ACS Applied Materials & Interfaces 10 (49):42826-42836

7. Yu XG, Li YQ, Zhu WB, Huang P, Wang TT, Hu N, Fu SY (2017) A wearable strain sensor based on a carbonized nano-sponge/silicone composite for human motion detection. Nanoscale 9 (20):6680

8. Wu H, Liu Q, Chen H, Shi G, Li C (2018) Fibrous strain sensor with ultra-sensitivity, wide sensing range, and large linearity for full-range detection of human motion. Nanoscale 10 (37):17512-17519

9. Li Y, Zhou B, Zheng G, Liu X, Li T, Yan C, Cheng C, Dai K, Liu C, Shen C, Guo Z (2018) Continuously prepared highly conductive and stretchable SWNT/MWNT synergistically composited electrospun thermoplastic polyurethane yarns for wearable sensing. Journal of Materials Chemistry C 6 (9):2258-2269

10. Ding Y, Yang J, Tolle CR, Zhu Z (2016) A Highly Stretchable Strain Sensor Based on Electrospun Carbon Nanofibers for Human Motion Monitoring. Rsc Advances 6 (82):79114-79120

11. Wang X, Meng S, Tebyetekerwa M, Li Y, Pionteck J, Sun B, Qin Z, Zhu M (2018) Highly sensitive and stretchable piezoresistive strain sensor based on conductive poly (styrene-butadiene-styrene)/few layer graphene composite fiber. Composites Part A: Applied Science and Manufacturing 105:291-299

12. Costa P, Carvalho MF, Correia V, Viana JC, Lanceros-Méndez S (2018) Polymer Nanocomposite-Based Strain Sensors with Tailored Processability and Improved Device Integration. ACS Applied Nano Materials 1 (6):3015-3025

13. Khan H, Razmjou A, Ebrahimi WM, Kottapalli A, Asadnia M (2018) Sensitive and Flexible Polymeric Strain Sensor for Accurate Human Motion Monitoring. Sensors 18 (2):418

14. Li G, Dai K, Ren M, Wang Y, Zheng G, Liu C, Shen C (2018) Aligned flexible conductive fibrous networks for highly sensitive, ultrastretchable and wearable strain sensors. Journal of Materials Chemistry C 6 (24):6575-6583

15. Liu Y, Zheng H, Liu M (2017) High performance strain sensors based on chitosan/carbon black composite sponges. Materials & Design 141:276-285

16. Darbandi SMA, Nouri M (2012) Electrospun nanostructures based on polyurethane/MWCNTs for strain sensing applications. Fibers & Polymers 13 (9):1126-1131

17. Fu X, Aljumaily AM, Ramos M, Meshkinzar A, Huang X (2019) Stretchable and sensitive sensor based on carbon nanotubes/polymer composite with serpentine shapes via molding technique. Journal of Biomaterials Science-polymer Edition 30 (13):1227-1241

18. Sun B, Long Y-Z, Chen Z-J, Liu S-L, Zhang H-D, Zhang J-C, Han W-P (2014) Recent advances in flexible and stretchable electronic devices via electrospinning. Journal of Materials Chemistry C 2 (7):1209-1219

19. Wang X, Sun H, Yue X, Yu Y, Zheng G, Dai K, Liu C, Shen C (2018) A highly

stretchable carbon nanotubes/thermoplastic polyurethane fiber-shaped strain sensor with porous structure for human motion monitoring. Composites Science and Technology 168:126-132

20. Jiang L, Zhou Y, Wang Y, Jiang Z, Zhou F, Chen S, Ma J (2018) Fabrication of Dielectric Elastomer Composites by Locking a Pre-Stretched Fibrous TPU Network in EVA. Materials 11 (9):1687

21. Lu L, Wei X, Zhang Y, Zheng G, Dai K, Liu C, Shen C (2017) A flexible and self-formed sandwich structure strain sensor based on AgNW decorated electrospun fibrous mats with excellent sensing capability and good oxidation inhibition properties. Journal of Materials Chemistry C 5 (28):7035-7042

22. Tong L, Wang XX, He XX, Nie GD, Zhang J, Zhang B, Guo WZ, Long YZ (2018) Electrically Conductive TPU Nanofibrous Composite with High Stretchability for Flexible Strain Sensor. Nanoscale Research Letters 13 (1):86

23. Yang K, Yin F, Xia D, Peng H, Yang J, Yuan W (2019) A highly flexible and multifunctional strain sensor based on a network-structured MXene/polyurethane mat with ultra-high sensitivity and a broad sensing range. Nanoscale 11 (20):9949-9957

24. Lee KH, Kim KW, Pesapane A, Kim HY, Rabolt JF (2008) Polarized FT-IR Study of Macroscopically Oriented Electrospun Nylon6 Nanofibers. Macromolecules 41 (4):1494-1498

25. Yusuf Y, Ula NM, Jahidah K, Kusumasari EM, Triyana K, Sosiati H, Harsojo (2016) Study of parallel oriented electrospun polyvinyl alcohol (PVA) nanofibers using modified electrospinning method. AIP Conference Proceedings 1725 (1):020104

26. Mei L, Song P, Liu Y (2015) Magnetic-field-assisted electrospinning highly aligned composite nanofibers containing well-aligned multiwalled carbon nanotubes. Journal of Applied Polymer Science 132 (22):41995

27. Liu Z, Pan CT, Lin L, Huang JC, Ou Z (2014) Direct-write PVDF nonwoven fiber fabric energy harvesters via the hollow cylindrical near-field electrospinning process. Smart Materials and Structures 23 (2):025003

28. Ma S, Ye T, Zhang T, Wang Z, Li K, Chen M, Zhang J, Wang Z, Ramakrishna S, Wei L (2018) Highly Oriented Electrospun P (VDF-TrFE) Fibers via Mechanical Stretching for Wearable Motion Sensing. Advanced Materials Technologies 3 (7):1800033

29. Jiang Y, Gong L, Hu X, Zhao Y, Chen H, Feng L, Zhang D (2018) Aligned P (VDF-TrFE) nanofibers for enhanced piezoelectric directional strain sensing. Polymers 10 (4):364

30. Chang-Mou W, Min-Hui C, Wun-Yuan Z (2018) Piezoelectric Response of Aligned Electrospun Polyvinylidene Fluoride/Carbon Nanotube Nanofibrous Membranes. Nanomaterials 8 (6):420

31. Zhao D, Zhang Q, Liu Y, Zhang Y, Guo X, Yuan Z, Zhang W, Zhang R, Lian JW, Sang S (2019) Highly sensitive and flexible strain sensor based on AuNPs/CNTs' synergic conductive network. Applied Nanoscience 9 (7):1469-1478

32. Yu S, Wang X, Xiang H, Zhu L, Tebyetekerwa M, Zhu M (2018) Superior piezoresistive strain sensing behaviors of carbon nanotubes in one-dimensional polymer fiber structure. Carbon 140:1-9

33. Jiang L, Kennedy D, Jerrams S, Betts A (2016) Enhancement of dielectric properties with the addition of bromine and dopamine modified barium titanate particles to silicone rubber. MRS Communications 6 (4):437-441

34. Knorr DB, Tran NT, Gaskell KJ, Orlicki JA, Woicik JC, Jaye C, Fischer DA, Lenhart JL (2016) Synthesis and Characterization of Aminopropyltriethoxysilane-Polydopamine Coatings. Langmuir 32 (17):4370-4381

35. Li X, Shan H, Cao M, Li B (2018) Mussel-inspired modification of PTFE membranes in a miscible THF-Tris buffer mixture for oil-in-water emulsions separation. Journal of Membrane Science 555:237-249.

36. Pan H, Li L, Hu L, Cui X (2006) Continuous aligned polymer fibers produced by a modified electrospinning method. Polymer 47 (14):4901-4904

37. Sundaray B, Subramanian V, Natarajan TS, Xiang R-Z, Chang C-C, Fann W-S (2004) Electrospinning of continuous aligned polymer fibers. Applied Physics Letters 84 (7):1222-1224

38. Fennessey SF, Farris RJ (2004) Fabrication of aligned and molecularly oriented electrospun polyacrylonitrile nanofibers and the mechanical behavior of their twisted yarns. Polymer 45 (12):4217-4225

39. Lee J, Deng Y (2012) Increased mechanical properties of aligned and isotropic electrospun PVA nanofiber webs by cellulose nanowhisker reinforcement. Macromolecular research 20 (1):76-83

40. Nitti P, Gallo N, Natta L, Scalera F, Palazzo B, Sannino A, Gervaso F (2018) Influence of Nanofiber Orientation on Morphological and Mechanical Properties of

Electrospun Chitosan Mats. Journal of Healthcare Engineering 2018:1-12

41. Wong SCJ, Baji A, Leng S (2008) Effect of Fiber Diameter on Tensile Properties of Electrospun Poly(ε-Caprolactone). Polymer 49 (21):4713-4722

42. Yuan H, Zhou Q, Zhang Y (2017) Improving fiber alignment during electrospinning. In: Electrospun Nanofibers. Elsevier, pp 125-147

43. Ma S, Li H, Chen H, Chen S, Ding Y, Yang W (2014) Hydrophilic modification of ultrafine fibres produced by melt differential electrospinning device. Materials Research Innovations 18 (4):914-920

44. Huang F, Wei Q, Cai Y, Ning W (2008) Surface Structures and Contact Angles of Electrospun Poly(vinylidene fluoride) Nanofiber Membranes. International Journal of Polymer Analysis & Characterization 13 (4):292-301

45. Song Y, Shen Y, Liu H, Lin Y, Li M, Nan CW (2012) Enhanced Dielectric and Ferroelectric Properties Induced by Dopamine-Modified $BaTiO_3$ Nanofibers in Flexible Poly(Vinylidene Fluoride-Trifluoroethylene) Nanocomposites. Journal of Materials Chemistry 22 (16):8063-8068

46. Gao J, Li W, Shi H, Hu M, Li RKY (2014) Preparation, morphology, and mechanical properties of carbon nanotube anchored polymer nanofiber composite. Composites Science and Technology 92:95-102

47. Liu L, Huang YD, Zhang Z, Jiang ZX, Wu L (2008) Ultrasonic treatment of aramid fiber surface and its effect on the interface of aramid/epoxy composites. Applied Surface Science 254 (9):2594-2599

48. Ren M, Zhou Y, Wang Y, Zheng G, Dai K, Liu C, Shen C (2019) Highly stretchable

and durable strain sensor based on carbon nanotubes decorated thermoplastic polyurethane fibrous network with aligned wave-like structure. Chemical Engineering Journal 360:762-777

49. Yusoff NIM, Chailleux E, Airey GD (2011) A Comparative Study of the Influence of Shift Factor Equations on Master Curve Construction. International journal of pavement research and technology 4 (6):324-336